

# PCCP

Accepted Manuscript



This is an *Accepted Manuscript*, which has been through the Royal Society of Chemistry peer review process and has been accepted for publication.

*Accepted Manuscripts* are published online shortly after acceptance, before technical editing, formatting and proof reading. Using this free service, authors can make their results available to the community, in citable form, before we publish the edited article. We will replace this *Accepted Manuscript* with the edited and formatted *Advance Article* as soon as it is available.

You can find more information about *Accepted Manuscripts* in the [Information for Authors](#).

Please note that technical editing may introduce minor changes to the text and/or graphics, which may alter content. The journal's standard [Terms & Conditions](#) and the [Ethical guidelines](#) still apply. In no event shall the Royal Society of Chemistry be held responsible for any errors or omissions in this *Accepted Manuscript* or any consequences arising from the use of any information it contains.



Journal Name

ARTICLE

## Strength order and nature of the $\pi$ -hole bond of cyanuric chloride and 1,3,5-triazine with halide

Hui Wang,<sup>a</sup> Chen Li,<sup>a</sup> Weizhou Wang,<sup>\*b</sup> Wei Jun Jin<sup>\*a</sup>Received 00th January 20xx,  
Accepted 00th January 20xx

DOI: 10.1039/x0xx00000x

www.rsc.org/

The <sup>13</sup>C NMR chemical shift moving to higher field indicated main  $\pi$ -hole...X<sup>-</sup> bonding model between cyanuric chloride/1,3,5-triazine (3CIN/3N) processing both  $\pi$ -hole and  $\sigma$ -hole and X<sup>-</sup>. The <sup>13</sup>C NMR and UV adsorption titration in acetonitrile confirmed that the bonding abilities of 3CIN/3N with X<sup>-</sup> obeys the order I<sup>-</sup> > Br<sup>-</sup> > Cl<sup>-</sup>, which seems apparently to be the order of charge transfer ability of halide to 3CIN/3N. The calculation chemistry showed that the bonding abilities in solution phase were essentially consistent with that obtained by titration experiments. However, the results in gas phase were contrary, *i.e.*,  $\pi$ -hole...Cl<sup>-</sup> >  $\pi$ -hole...Br<sup>-</sup> >  $\pi$ -hole...I<sup>-</sup> in bonding energy, which obey the order of electrostatic interaction. In fact, the  $\pi$ -hole bond and  $\sigma$ -hole bond compete with solvation and possible anion-hydrogen bond between solvent molecule and halide in solution. A tradeoff is that the apparent charge transfer order of  $\pi$ -/ $\sigma$ -hole...I<sup>-</sup> >  $\pi$ -/ $\sigma$ -hole...Br<sup>-</sup> >  $\pi$ -/ $\sigma$ -hole...Cl<sup>-</sup> occurs for weak  $\pi$ -hole bond and  $\sigma$ -hole bond, while really electrostatic attractive order of  $\pi$ -/ $\sigma$ -hole...Cl<sup>-</sup> >  $\pi$ -/ $\sigma$ -hole...Br<sup>-</sup> >  $\pi$ -/ $\sigma$ -hole...I<sup>-</sup> works for strong ones. It can be concluded by combining the energy decomposition analysis and natural bond orbital analysis that the  $\pi$ -hole...X<sup>-</sup> bond and  $\sigma$ -hole...X<sup>-</sup> bond are electrostatically attractive in nature regardless of the order of I<sup>-</sup> > Br<sup>-</sup> > Cl<sup>-</sup> or converse.

### Introduction

Anion recognition is one of the important themes in supramolecular chemistry during the past several decades.<sup>1,2</sup> Two promising bonding interactions, the  $\sigma$ -hole bond and  $\pi$ -hole bond, are being garnering much attention in recent years.<sup>3-6</sup> The  $\sigma$ -hole bond refers to the interaction between the positive surface electrostatic potential (SEP) region of a molecule entity along extensions of Y-X/S/P/Ge/H covalent  $\sigma$ -bond/s (Y: electron-rich group; X/S/P/Ge/H: halogen, chalcogen, pnictogen, silicon and hydrogen, respectively) and negative site. Halogen bond, chalcogen bond, pnictogen bond, silicon bond or hydrogen bond, is only a subset of  $\sigma$ -hole bond.<sup>3,7</sup> Similarly, the  $\pi$ -hole bond refers to the interaction between the region with positive SEP in the direction perpendicular to the  $\sigma$ -framework of the aromatic or non-aromatic molecular entity and negative site. At present, halogen bond as the representative of the  $\sigma$ -hole bond, and the  $\pi$ -hole bond all have been shown to exhibit great advantages and a great progress has been made in anion recognition.<sup>8-11</sup> However, the nature and interplay of the  $\sigma$ -hole bond and  $\pi$ -hole bond, as well as the effect of solvent

polarity, anion-hydrogen bond between solvent molecule and halide on their ability, *etc.*, have been closely concerned topics (the anion-hydrogen bond between solvent molecule and halide also can name the  $\sigma$ -hole...anion bond. But in order to avoid confusion, it named still hydrogen bond).

The nature of two bonds can be analyzed qualitatively by the SEP of molecule and energy decomposition analysis. In general, stronger  $\sigma$ -hole bonding and  $\pi$ -hole bonding complexes are more likely to be formed as the SEP of the  $\sigma$ -hole and  $\pi$ -hole become more positive. The energy decomposition analysis (EDA) has provided great supports for insight into the physical origin of two bonding models by decomposing the total interaction energy into physically meaningful components, such as electrostatic energy ( $E_{\text{elst}}$ ), dispersive force ( $E_{\text{disp}}$ ), induction interaction ( $E_{\text{ind}}$ ) and other weak effects, *etc.* It has been revealed for the nature of the  $\sigma$ -hole bond and  $\pi$ -hole bond that the electrostatic attraction is dominant in most cases (the proportion of  $E_{\text{elst}}$  is 51% – 72%),<sup>12-16</sup> while in some cases, the electrostatic and polarization/induction terms dominate, the proportions of  $E_{\text{elst}}$  and  $E_{\text{pol}}/E_{\text{ind}}$  are 49% – 67% and 31% – 51%,<sup>17,18</sup> or 33% – 40% and 33% – 50%,<sup>19-21</sup> respectively. In a few cases, the charge-transfer or orbital terms (the proportion of  $E_{\text{oi}}$  is 47% – 72%)<sup>22</sup> are dominant. However, for weak bonding complexes, dispersion, polarization/induction, or dispersion and induction are dominant.<sup>23-25</sup> In a word, the main driving force is somewhat different in different decomposition schemes and different interaction systems.

<sup>a</sup> College of Chemistry, Beijing Normal University, Beijing 100875, P. R. China.  
Tel/Fax: (+86)10-58802146, E-mail: wjjin@bnu.edu.cn

<sup>b</sup> College of Chemistry and Chemical Engineering, Luoyang Normal University,  
Luoyang 471022, P. R. China. E-mail: wzw@lynu.edu.cn

† Electronic Supplementary Information (ESI) available: [The Figure and Tables of NBO calculation]. See DOI: 10.1039/x0xx00000x

Herein, cyanuric chloride (3CIN) and 1,3,5-triazine (3N) possessing both the  $\pi$ -hole and  $\sigma$ -hole were selected as donor molecules to study their bonding abilities with different halide anions in solution. The  $^{13}\text{C}$  NMR chemical shift moving to the higher field indicated that the main bonding model was  $\pi$ -hole $\cdots\text{X}^-$  bond between 3CIN/3N and  $\text{X}^-$ . The UV absorption and  $^{13}\text{C}$  NMR titration methods all indicated that the bonding abilities of 3CIN/3N with  $\text{X}^-$  decreased in the order  $\pi$ -hole $\cdots\text{I}^- > \pi$ -hole $\cdots\text{Br}^- > \pi$ -hole $\cdots\text{Cl}^-$ . The bonding abilities in solution phase evaluated by computational chemistry were essentially consistent with that obtained by titration experiments, but the calculated bonding order in gas phase are different from them obtained by experiments. It is ascribed to the strong solvation of halide. In addition, SAPT energy decomposition combining with NBO analysis supports the nature of electrostatic attraction of both the  $\pi$ -hole $\cdots\text{X}^-$  bond and  $\sigma$ -hole $\cdots\text{X}^-$  bond.

## Experimental

### Materials

Cyanuric chloride (3CIN, 99%) was purchased from J&K Co. (Beijing, China). 1,3,5-triazine (3N, 95%), tetrapropylammonium chloride ( $\text{Pr}_4\text{N}^+\text{Cl}^-$ , 98%), tetrapropylammonium bromide ( $\text{Pr}_4\text{N}^+\text{Br}^-$ , 98%) and tetrapropylammonium iodide ( $\text{Pr}_4\text{N}^+\text{I}^-$ , 98%) were purchased from TCI Co. (Tokyo, Japan). Acetonitrile-D3 was purchased from Merck Co. (Darmstadt, Germany). Acetonitrile (99.5%) was supplied by Tianjin Bodi Chemical Co. (Tianjin, China) and was dried on  $\text{CaH}_2$  to use. All the other reagents are of analytical purity grade and used without further purification.

### Spectroscopic measurements

The UV adsorption spectra were recorded by an incremental addition of  $\text{X}^-$  (from 0.10 to 0.96 M) to 3 mM 3CIN or 20 mM 3N solution using 1-mm quartz cuvette on a TU-1901 spectrophotometer (Beijing Purkinje General Instrument Co. LTD). The associate constant ( $K_a$ ) and molar absorption coefficient ( $\epsilon$ ) were obtained by UV titration method. The  $^{13}\text{C}$  NMR spectra were recorded using a Bruker Avance III 400 MHz NMR Spectrometer (Bruker Corporation, Billerica, MA, USA).

### Computational Methods

The structures of all monomers and complexes in gas and solution phase were fully optimized using the density functional M06-2X.<sup>26</sup> The basis set 6-311++G(d,p) was used for describe C, H, N, Cl, Br atoms and 6-311++G(d,p)/LANL2DZdp ECP for I atom. All the structures were confirmed as true minima on the potential energy surfaces by the presence of only real frequencies after the corresponding vibrational analysis at the same theory level. It should be noticed that Alkorta and Frontera tested the performance of pure and hybrid DFT methods for the halogen, chalcogen, and pnictogen bonds involving anionic and neutral electron donors, and concluded that, "apart from the M06-2X method, all other DFT and MP2 *ab initio* methods largely overestimate the halogen bonding interaction when the donor is anion".<sup>27</sup> The interaction energy ( $\Delta E$ ) of each complex is calculated as the difference between the energy of the complex and the sum of total energies of the monomers  $\Delta E_{\text{total}} = E_{\text{AB}} - (E_{\text{A}} +$

$E_{\text{B}})$ . The basis set superposition error (BSSE) is estimated using counterpoise (CP) method of Boys-Bernardi. Fully optimized calculations in solution are performed via the standard polarizable continuum model (PCM).<sup>28</sup>

In order to understand the nature of  $\sigma$ -hole bond and  $\pi$ -hole bond, the EDA of the complexes in gas phase is completed using symmetry-adapted perturbation theory (SAPT) method<sup>29,30</sup> with aug-cc-pVDZ basis set. The theory of the SAPT method can be found elsewhere.<sup>23</sup> Furthermore, the optimized geometries were then used to perform natural bond orbital (NBO) analysis<sup>31</sup> from NBO program. Density functional theory calculations and NBO analyses were carried out with GAUSSIAN09 quantum chemistry package.<sup>32</sup> SAPT calculations were performed using MOLPRO quantum chemistry package.<sup>33</sup>

## Results and discussion

### The molecular surface electrostatic potentials (SEP)

Fig. 1 shows the SEP of 3CIN and 3N calculated at M06-2X/6-311++G(d,p) level. Both 3CIN and 3N molecules possess the  $\pi$ -hole and  $\sigma$ -hole: the maximum value ( $V_{s,\text{max}}$ ) of positive SEP in the direction perpendicular to the  $\sigma$ -framework of the molecule entities are 143.8 and 75.6  $\text{kJ}\cdot\text{mol}^{-1}$ , and on the region of molecule entities along extensions of C-Cl/H covalent bonds are 81.3 and 96.4  $\text{kJ}\cdot\text{mol}^{-1}$ , respectively. Therefore, it can be predicted that 3CIN/3N and  $\text{X}^-$  can not only form the  $\pi$ -hole bond, but also form the  $\sigma$ -hole bond (halogen or hydrogen bond). In addition, according to the  $V_{s,\text{max}}$ , it can also be predicted that 3CIN and  $\text{X}^-$  are prone to form the  $\pi$ -hole bond, while 3N and  $\text{X}^-$  are prone to form the  $\sigma$ -hole bond (hydrogen bond). It can be expected that the recognition of halide anion is possible by the  $\pi$ -hole bond or  $\sigma$ -hole bond using the 3CIN and 3N in solution. This will be discussed specifically in the following part through UV absorption spectra,  $^{13}\text{C}$  NMR and computational chemistry.

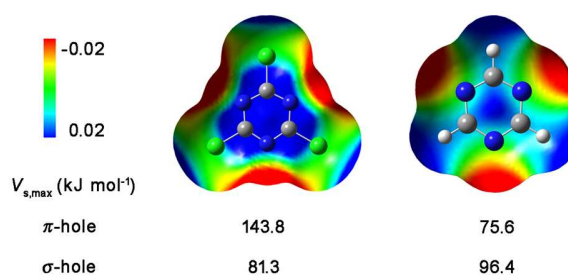


Fig. 1 The SEP of 3CIN and 3N molecules calculated at the M06-2X/6-311++G(d,p) level.

### The determination of association constant and bonding model

The determination of association constant is a very important part in anion recognition based on supramolecular chemistry for quantitatively understanding the relevant bonding interactions. Herein, association constants between 3CIN/3N and halide are obtained and the specific bonding models are confirmed by UV spectra and  $^{13}\text{C}$  NMR titration experiments combining with computational chemistry, which provided

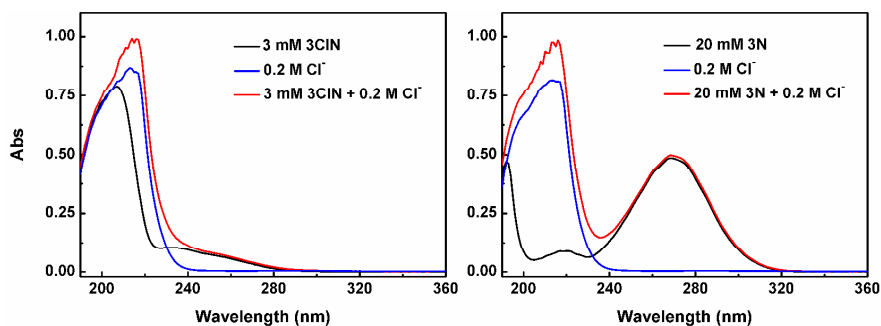


Fig. 2 The UV absorption spectra of 3CIN/3N,  $\text{Cl}^-$  (as an example of halide anion) and their mixture in acetonitrile.

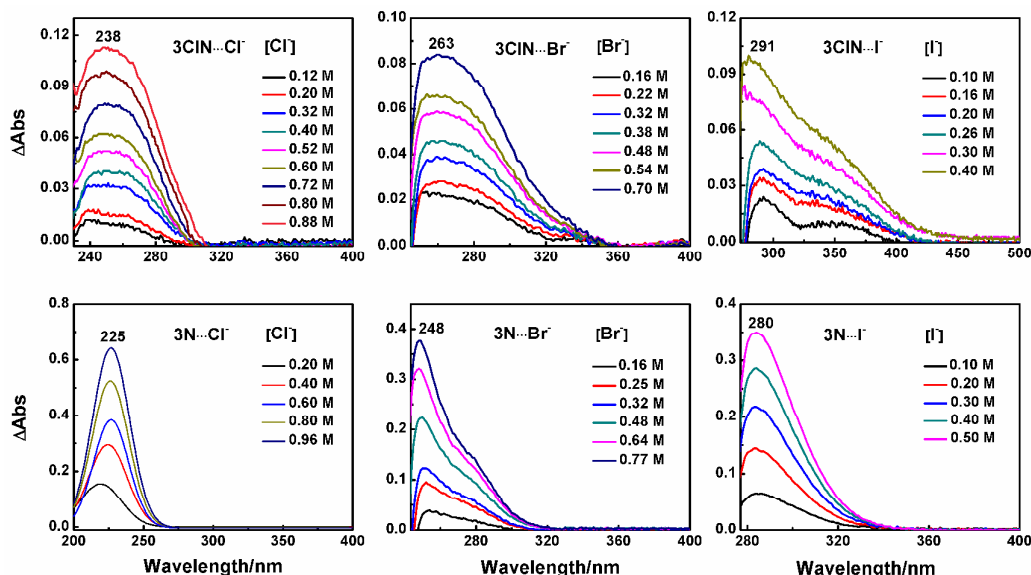


Fig. 3 The Pure UV absorption spectra of  $3\text{CIN}\cdots\text{X}^-$  (top) and  $3\text{N}\cdots\text{X}^-$  (bottom) complexes obtained by the subtracted spectrum with increasing  $[\text{X}^-]$  in acetonitrile by setting the concentration of 3CIN and 3N at 3 mM and 20 mM, respectively.

useful information for the recognition abilities of 3CIN and 3N to halide anions.

#### UV absorption spectrum titration

In this experiment, the UV absorption spectra of mixture are obtained by an incremental addition of  $\text{X}^-$  (from 0.10 to 0.96 M) into 3 mM 3CIN or 20 mM 3N solution. Acetonitrile is selected as the solvent because of its desirable ability to dissolve both donors and acceptors with high solubility and its little background in the UV absorption spectrum.

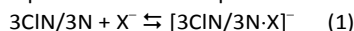
Fig. 2 shows the primitive absorption spectra of 3CIN/3N,  $\text{Cl}^-$  and their mixture in acetonitrile. The absorption bands of 3CIN and 3N are located at 207, 269 nm and 192, 218, 269 nm, respectively. There is not very sharp change in spectrum to show the formation of the  $3\text{CIN}\cdots\text{Cl}^-$  and  $3\text{N}\cdots\text{Cl}^-$  bonding complexes when a certain concentration of  $\text{Cl}^-$  is added to 3 mM 3CIN and 20 mM 3N solution. In order to observe very salient bands of complexes and eliminate the overlay from the absorption of monomer species 3CIN, 3N and  $\text{X}^-$ , the subtracted spectrum is obtained by subtracting the spectrum of both 3CIN/3N and  $\text{X}^-$  from that of the mixture. The

absorption bands of new complexes are clearly observed from the subtracted spectrum; moreover, they are enhanced gradually with increasing  $[\text{X}^-]$  (cf. Fig. 3).

As can be seen from Fig. 3, the  $\lambda_{\text{max}}$  values are 238 nm ( $3\text{CIN}\cdots\text{Cl}^-$ ), 263 nm ( $3\text{CIN}\cdots\text{Br}^-$ ) and 291 nm ( $3\text{CIN}\cdots\text{I}^-$ ) for  $3\text{CIN}\cdots\text{X}^-$  complex; 225 nm ( $3\text{N}\cdots\text{Cl}^-$ ), 248 nm ( $3\text{N}\cdots\text{Br}^-$ ) and 280 nm ( $3\text{N}\cdots\text{I}^-$ ) for  $3\text{N}\cdots\text{X}^-$  complex, respectively. The difference of  $\lambda_{\text{max}}$  in the same donor with various acceptors is related to the relevant electron transfer energy from  $\text{X}^-$  to 3CIN and 3N molecules, which can be reflected intuitively from Mulliken correlation<sup>34,35</sup> related with charge transfer theory. According to this theory, the transition energy between electron donor and electron acceptor is primarily determined by the energy difference of HOMO/LUMO that can be evaluated by the redox potential in solution. The oxidation waves of halide anion in  $\text{CH}_3\text{CN}$  were 1.050 V ( $\text{Cl}^-$ ), 0.710 V ( $\text{Br}^-$ ) and 0.378 V ( $\text{I}^-$ ), respectively.<sup>36</sup> Therefore, the absorption energy of complexes sharing the same electron acceptor (the  $\pi$ -hole and  $\sigma$ -hole bonding donor, 3CIN or 3N) must be linear correlation with the oxidation potential of different electron donors ( $\text{X}^-$ ), and vice

versa. Fig. 4a shows that the absorption energies of complexes (in  $\text{cm}^{-1}$ ) correlate well with the oxidation potentials of  $X^-$  (correlation coefficient  $R^2 = 0.999$  for  $3\text{CIN}\cdots X^-$  complex and  $R^2 = 0.997$  for  $3\text{N}\cdots X^-$  complex), which reveals that charge transfer term contributes to the interaction system.

If the  $3\text{CIN}/3\text{N}\cdots X^-$  complexes have 1:1 stoichiometry, the complexation can be expressed as follows:



The association constant  $K_a$  and molar absorption coefficient  $\varepsilon$  of the  $3\text{CIN}\cdots X^-$  and  $3\text{N}\cdots X^-$  complexes can be obtained by Benesi–Hildebrand methodology (Eq. 2).<sup>37</sup>

$$\frac{b[3\text{CIN}/3\text{N}]_0}{\Delta Abs} = \frac{1}{K_a \varepsilon [X^-]_0} + \frac{1}{\varepsilon} \quad (2)$$

Where  $b$  is the thickness of solution,  $\Delta Abs$  is the differential absorbance,  $[3\text{CIN}/3\text{N}]_0$  and  $[X^-]_0$  are the initial concentration of the donors and acceptors in  $\text{mol}\cdot\text{L}^{-1}$ , respectively.

The plots of  $[3\text{CIN}]/b/\Delta Abs$  and  $[3\text{N}]/b/\Delta Abs$  vs.  $1/[X^-]_0$  are linear according to Eq. 2 as illustrated in Fig. 4b and 4c. The correlation coefficients ( $R^2$ ) of the fitted straight lines are all greater than 0.99. The good linear relationship indicates that 3CIN and 3N form 1:1 complexes with different  $X^-$  in the tested concentration ranges. The association constants of the complexes are 0.172 ( $3\text{CIN}\cdots\text{Cl}^-$ ), 0.343 ( $3\text{CIN}\cdots\text{Br}^-$ ) and 1.004 ( $3\text{CIN}\cdots\text{I}^-$ )  $\text{M}^{-1}$  for 3CIN complexes, and 0.370 ( $3\text{N}\cdots\text{Cl}^-$ ), 0.688 ( $3\text{N}\cdots\text{Br}^-$ ) and 1.011 ( $3\text{N}\cdots\text{I}^-$ )  $\text{M}^{-1}$  for 3N complexes, as listed in Table 1. It can be concluded that the bonding abilities of both 3CIN and 3N to  $X^-$  obey the order of  $\text{I}^- > \text{Br}^- > \text{Cl}^-$ .

**Table 1** The spectroscopic characteristics and bonding constants of  $3\text{CIN}\cdots X^-$  and  $3\text{N}\cdots X^-$  complexes in acetonitrile.

Complexes	$\lambda_{\text{max}}/\text{nm}$	$\varepsilon/10^3\text{M}^{-1}\text{cm}^{-1}$	$K_a/\text{M}^{-1}$
$3\text{CIN}\cdots\text{Cl}^-$	238	$2.109 \pm 0.440$	$0.172 \pm 0.030$
$3\text{CIN}\cdots\text{Br}^-$	263	$1.433 \pm 0.210$	$0.343 \pm 0.110$
$3\text{CIN}\cdots\text{I}^-$	291	$0.856 \pm 0.120$	$1.004 \pm 0.170$
$3\text{N}\cdots\text{Cl}^-$	225	$0.231 \pm 0.021$	$0.370 \pm 0.070$
$3\text{N}\cdots\text{Br}^-$	248	$0.368 \pm 0.025$	$0.688 \pm 0.100$
$3\text{N}\cdots\text{I}^-$	280	$0.428 \pm 0.031$	$1.011 \pm 0.150$

$\varepsilon$  and  $K_a$  are the average results of triplicate.

The electronic absorption spectrum is a good method for investigating the weak intermolecular interaction, but it has a certain limitation in this system. It indeed confirms that 3CIN and 3N could interact with  $X^-$ . However, it is difficult to confirm which one of the  $\pi$ -hole $\cdots X^-$  and  $\sigma$ -hole $\cdots X^-$  bonds works, also to obtain the accurate geometry information of the complexes is not possible.

#### <sup>13</sup>C NMR titration

NMR spectroscopy is another powerful tool to probe the weak interaction. It can provide the complementary structural information (bonding model) which is not obtainable by UV–Vis absorption spectroscopy, and it can also evaluate the bonding ability of interactions between donors and acceptors.

The formation of the  $\sigma$ -hole bond changes the electron density around carbon atom bonded to the halogen or hydrogen atom remarkably. Shifting the electron toward other parts of the molecule deshields the nucleus of the carbon atom bonded to the halogen/hydrogen atom and causes an increase in the <sup>13</sup>C NMR chemical shift.<sup>38</sup> From the interpretation of orbital change, *i.e.*, Lewis acid–base interaction, namely mixing of Lewis base’s electron pair with the empty C–I  $\sigma^*$  orbital leads to increased paramagnetic deshield. Further paramagnetic deshielding effect comes from polarization of iodine  $p$  lone pairs onto carbon and it will move the chemical shift to lower frequency.<sup>39,40</sup> However, the formation of the  $\pi$ -hole bond will lead to the decrease of the chemical shift of the carbon atom, due to the increase of electron density.<sup>41</sup> Therefore, the bonding type of the interactions of 3CIN and 3N with  $X^-$  can be determined by two contrary phenomena.

Herein, the changing trends of <sup>13</sup>C chemical shift of 3CIN and 3N molecules with the increase of  $X^-$  concentration were determined, in which the concentration of 3CIN and 3N were set at 0.048 M and 0.25 M with a variation of  $X^-$  concentration from 0.06 M to 0.75 M. Fig. 5 shows the <sup>13</sup>C NMR spectra of 3CIN and 3N in the absence and presence of  $\text{Cl}^-$  along with the values of chemical shift change. Because of the structural symmetry, the 3CIN and 3N molecules have only one <sup>13</sup>C NMR peak, the corresponding values of chemical shift are 173.0 ppm and 166.9 ppm, respectively, under the experimental

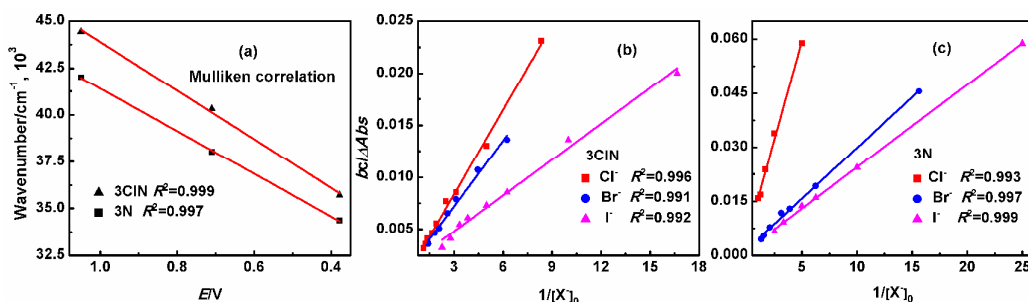


**Fig. 4** (a) Mulliken correlations between the wavenumbers of  $3\text{CIN}\cdots X^-$  and  $3\text{N}\cdots X^-$  complex bands and the oxidation potential of halide anion; (b) Benesi–Hildebrand plots of  $[3\text{CIN}]/b/\Delta Abs$  vs.  $1/[X^-]_0$ ; (c) Benesi–Hildebrand plots of  $[3\text{N}]/b/\Delta Abs$  vs.  $1/[X^-]_0$ .

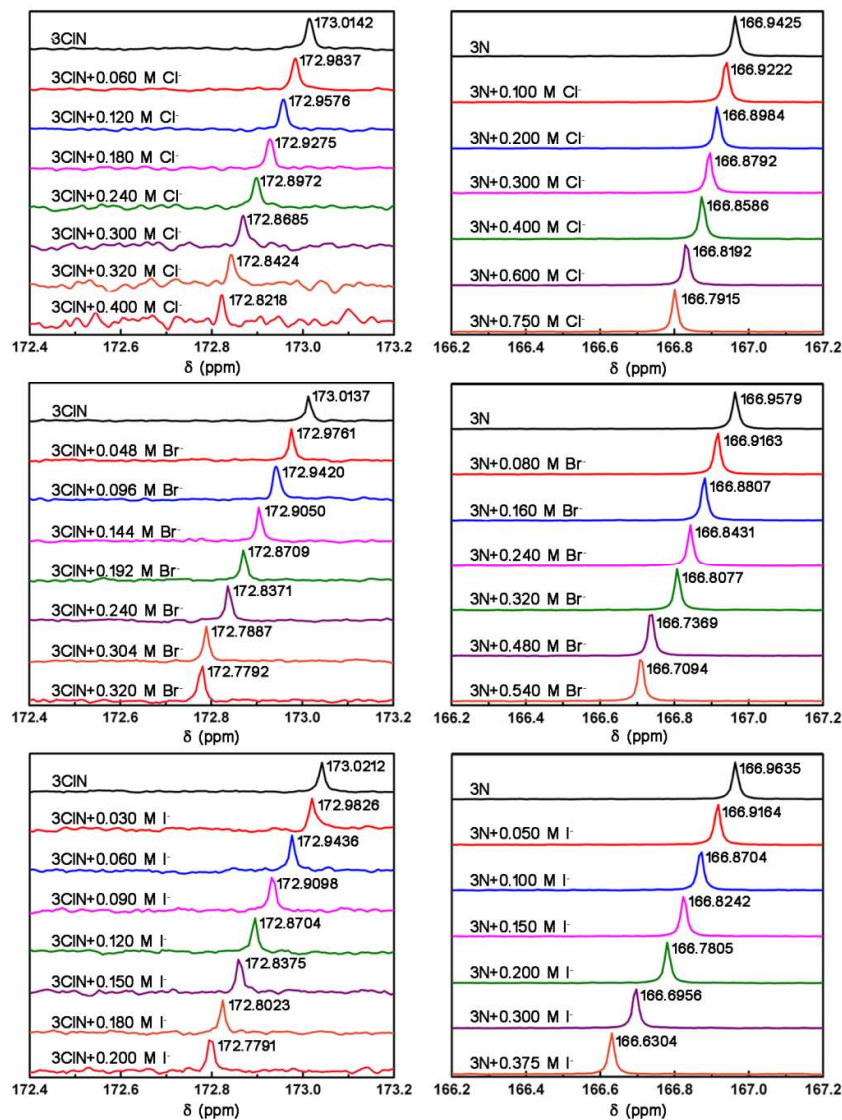


Fig. 5  $^{13}\text{C}$  NMR spectra of 3CIN (left) and 3N (right) in the absence and presence of  $\text{X}^-$  in acetonitrile- $\text{D}_3$  ( $[\text{3CIN}] = 0.048 \text{ M}$ ,  $[\text{3N}] = 0.25 \text{ M}$ ).

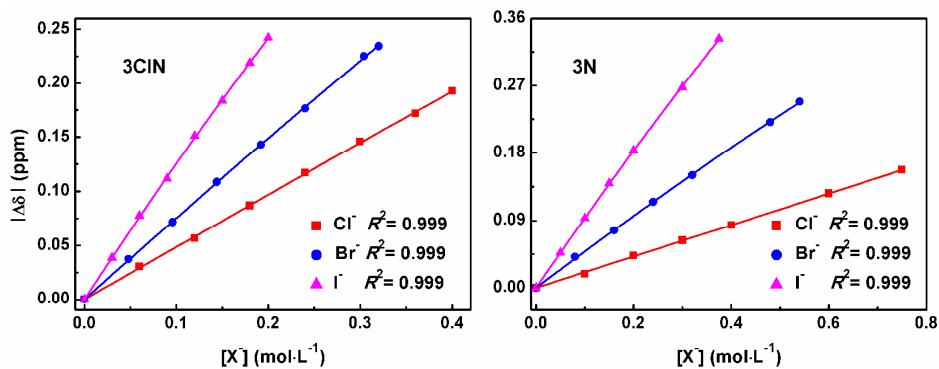


Fig. 6 The  $|\Delta\delta|$  of  $^{13}\text{C}$  NMR of 3CIN (left) and 3N (right) with the increase of concentration of  $\text{X}^-$  in acetonitrile- $\text{D}_3$  (The various dots refer to the experimental data and the curves refer to the results fitted by the Eq.3).

conditions. It can be observed that the  $^{13}\text{C}$  NMR chemical shifts of 3CIN and 3N move to the higher field, moreover, the varying amplitude of chemical shift is more obvious with the increase of  $\text{X}^-$  concentration. Therefore, it is reasonable to deduce that both 3CIN and 3N formed the  $\pi$ -hole $\cdots\text{X}^-$  bond rather than the  $\text{C}-\text{Cl}\cdots\text{X}^-$  or  $\text{C}-\text{H}\cdots\text{X}^-$   $\sigma$ -hole bond in acetonitrile.

As shown in Fig. 6, when the absolute values of the change in the  $^{13}\text{C}$  chemical shift ( $|\Delta\delta|$ ) of 3CIN and 3N molecules plotted against the concentration of  $\text{X}^-$ , it is found that the varying amplitude of  $^{13}\text{C}$  chemical shift decreases in the order of  $\text{I}^- > \text{Br}^- > \text{Cl}^-$  for the same  $\pi$ -hole bonding donor interacting with the same concentration of  $\text{X}^-$ . In other words, the higher the varying amplitude of  $^{13}\text{C}$  chemical shift, the stronger the formed  $\pi$ -hole $\cdots\text{X}^-$  bond is. The association constants  $K_a$  are obtained using nonlinear curve-fitting method (*i.e.*, Eq.3)<sup>42</sup> and listed in Table 2. It is shown obviously that the bonding abilities of 3CIN and 3N to  $\text{X}^-$  all follow the order  $\text{I}^- > \text{Br}^- > \text{Cl}^-$ , consistent with the result from UV spectrum titration.

$$\Delta\delta = \frac{\delta_{\text{DA}} - \delta_{\text{D}}}{2[\text{D}]_0} \left\{ [\text{D}]_0 + [\text{A}]_0 + 1/K_a - \sqrt{([\text{D}]_0 + [\text{A}]_0 + 1/K_a)^2 - 4[\text{D}]_0[\text{A}]_0} \right\} \quad (3)$$

Where  $[\text{D}]_0$ ,  $[\text{A}]_0$  is the initial concentration of the  $\pi$ -hole bonding donor and acceptor,  $[\text{DA}]$  is the equilibrium concentration of the formed  $\pi$ -hole bonding complexes,  $\delta_{\text{D}}$  and  $\delta_{\text{DA}}$  represents the  $^{13}\text{C}$  chemical shift of donor before and after adding the acceptor,  $K_a$  refers to the association constant.

**Table 2** The association constants of 3CIN $\cdots\text{X}^-$  and 3N $\cdots\text{X}^-$  complexes in acetonitrile–D<sub>2</sub>O by  $^{13}\text{C}$  NMR titration.

Complexes	$K_a/\text{M}^{-1}$	$R^2$
3CIN $\cdots\text{Cl}^-$	0.040	0.999
3CIN $\cdots\text{Br}^-$	0.115	0.999
3CIN $\cdots\text{I}^-$	0.401	0.999
3N $\cdots\text{Cl}^-$	0.131	0.999
3N $\cdots\text{Br}^-$	0.159	0.999
3N $\cdots\text{I}^-$	0.212	0.999

### Quantum chemistry calculation

#### Geometric parameters and interaction energies of the complexes

Although the bonding models and bonding abilities of the interactions of 3CIN and 3N with  $\text{X}^-$  are determined by UV and  $^{13}\text{C}$  NMR titrations, it is difficult to estimate the geometric structures of the complexes. Herein, the M06-2X method of density functional theory was used to simulate the possible bonding type and geometric structures of the complexes in gas phase and solution phase via the PCM model. For each complex, two bonding models were adopted, that is, the  $\pi$ -hole $\cdots\text{X}^-$  and  $\sigma$ -hole $\cdots\text{X}^-$  (halogen bond or hydrogen bond) bonding models. Fig. 7 shows the geometric structures of the complexes in gas phase, and the calculated geometric parameters and interaction energies ( $\Delta E$ ) are listed in Table 3.

**In gas phase**, it can be seen from the data in Table 3 that the interaction energies of the  $\pi$ -hole $\cdots\text{X}^-$  bonds ( $-52.7$  –  $-69.8$   $\text{kJ}\cdot\text{mol}^{-1}$ ) are greater than that corresponding  $\sigma$ -hole $\cdots\text{X}^-$  bonds ( $\text{C}-\text{Cl}\cdots\text{X}^-$  halogen bond,  $-28.4$  –  $-41.1$   $\text{kJ}\cdot\text{mol}^{-1}$ ) in the system of 3CIN $\cdots\text{X}^-$  complex, indicating that the main bonding model is the  $\pi$ -hole $\cdots\text{X}^-$  bond for the interactions of 3CIN with  $\text{X}^-$ . While in the 3N $\cdots\text{X}^-$  complexes, the interaction energies of the  $\sigma$ -hole $\cdots\text{X}^-$  bonds ( $\text{C}-\text{H}\cdots\text{X}^-$  hydrogen bond,  $-24.7$  –  $-37.8$   $\text{kJ}\cdot\text{mol}^{-1}$ ) are slightly greater than that corresponding  $\pi$ -hole $\cdots\text{X}^-$  bonds ( $-23.8$  –  $-32.5$   $\text{kJ}\cdot\text{mol}^{-1}$ ). That is, the  $\sigma$ -hole $\cdots\text{X}^-$  bond is slightly stronger than the  $\pi$ -hole $\cdots\text{X}^-$  bond in the 3N $\cdots\text{X}^-$  system based on calculation results. All these results are consistent with that predicted from the molecular SEP. Importantly, the interaction strengths between 3CIN/3N and  $\text{X}^-$  all decrease in the order  $\text{Cl}^- > \text{Br}^- > \text{I}^-$ , indicating that the primary driving force obeys an electrostatic attraction sequence.

**In solution phase**, the calculated interaction energies of complexes in solution phase are much smaller than that in gas phase. The interaction energies of the  $\pi$ -hole $\cdots\text{X}^-$  bonds ( $-18.7$  –  $-22.2$   $\text{kJ}\cdot\text{mol}^{-1}$ ) are also much greater than the corresponding  $\sigma$ -hole $\cdots\text{X}^-$  bonds ( $-5.4$  –  $-7.5$   $\text{kJ}\cdot\text{mol}^{-1}$ ) in the system of 3CIN $\cdots\text{X}^-$  complexes. However, in the 3N $\cdots\text{X}^-$  system, the interaction energies of the  $\pi$ -hole $\cdots\text{X}^-$  bonds ( $-6.6$  –  $-10.3$   $\text{kJ}\cdot\text{mol}^{-1}$ ) are slightly greater than that corresponding  $\sigma$ -hole $\cdots\text{X}^-$  bonds ( $-4.8$  –  $-7.1$   $\text{kJ}\cdot\text{mol}^{-1}$ ). In a word, the bonding strength of 3CIN and 3N with  $\text{X}^-$  in solution are basically identical with the experimental results, *i.e.*,  $\text{I}^- > \text{Br}^-$  or  $\text{Cl}^-$ , apparently an order of charge transfer ability of halide to 3CIN/3N.

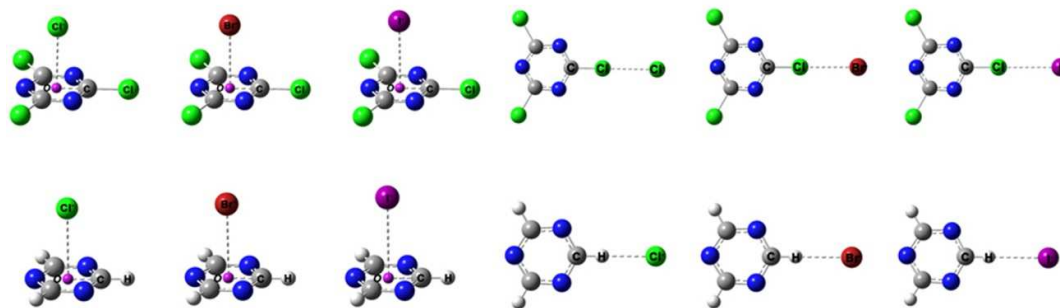


**Fig. 7** The interaction models and geometry of 3CIN $\cdots\text{X}^-$  and 3N $\cdots\text{X}^-$  complexes in gas phase. The small purple ball on molecular  $\sigma$ -framework plane presents the  $\pi$ -hole center.

**Table 3** The key geometrical parameters (bonding length in Å and bonding angle in °) and the corrected interaction energies ( $\Delta E$ , in  $\text{kJ}\cdot\text{mol}^{-1}$ ) of  $\pi$ -hole bond and  $\sigma$ -hole bond (halogen bond or hydrogen bond) in gas phase (Gas) and solution phase (Solution) calculated at the M06-2X/6-311++G(d,p)/LANL2DZdp ECP level, and the PCM solvent model was used in solution phase.

		$\pi$ -hole...X <sup>-</sup> bonding model			$\sigma$ -hole...X <sup>-</sup> bonding model		
		$d_{O-X}$	$\angle C-O...X$	$\Delta E$	$d_{Cl/H...X}$	$\angle C-Cl/H...X$	$\Delta E$
Gas	3CIN...Cl <sup>-</sup>	2.963	89.4	-69.8	3.027	180.0	-41.1
	3CIN...Br <sup>-</sup>	3.118	89.5	-61.5	3.148	180.0	-35.0
	3CIN...I <sup>-</sup>	3.381	89.8	-52.7	3.369	180.0	-28.4
	3N...Cl <sup>-</sup>	3.175	88.6	-32.5	2.341	180.0	-37.8
	3N...Br <sup>-</sup>	3.347	88.7	-27.8	2.502	180.0	-31.4
	3N...I <sup>-</sup>	3.651	88.8	-23.8	2.773	180.0	-24.7
Solution	3CIN...Cl <sup>-</sup>	3.158	87.9	-20.2	3.341	175.1	-6.0
	3CIN...Br <sup>-</sup>	3.351	87.7	-18.7	3.501	180.0	-5.4
	3CIN...I <sup>-</sup>	3.603	87.8	-22.2	3.708	180.0	-7.5
	3N...Cl <sup>-</sup>	3.439	89.6	-7.2	2.595	179.6	-5.6
	3N...Br <sup>-</sup>	3.578	89.3	-6.6	2.771	180.0	-4.8
	3N...I <sup>-</sup>	3.766	89.6	-10.3	2.985	180.0	-7.1

**Table 4** The interaction energies ( $E_{\text{SAPT}}$ ) and their decomposition into the electrostatic ( $E_{\text{elst}}$ ), exchange-repulsion ( $E_{\text{exch}}$ ), induction ( $E_{\text{ind}}$ ), and dispersion ( $E_{\text{disp}}$ ) terms; all in  $\text{kJ}\cdot\text{mol}^{-1}$ .

	$\pi$ -hole...X <sup>-</sup> bonding model					$\sigma$ -hole...X <sup>-</sup> bonding model				
	$E_{\text{elst}}$	$E_{\text{exch}}$	$E_{\text{ind}}$	$E_{\text{disp}}$	$E_{\text{SAPT}}$	$E_{\text{elst}}$	$E_{\text{exch}}$	$E_{\text{ind}}$	$E_{\text{disp}}$	$E_{\text{SAPT}}$
3CIN...Cl <sup>-</sup>	-83.60	77.07	-33.14	-28.16	-68.20	-52.72	60.21	-25.65	-13.26	-42.05
	57.7%		22.9%	19.4%		57.5%		28.0%	14.5%	
3CIN...Br <sup>-</sup>	-77.78	76.19	-28.20	-28.70	-58.62	-46.28	54.73	-20.75	-12.84	-34.73
	57.8%		20.9%	21.3%		57.9%		26.0%	16.1%	
3CIN...I <sup>-</sup>	-67.57	68.78	-22.22	-27.86	-47.78	-38.16	46.19	-15.69	-11.92	-26.69
	57.4%		18.9%	23.7%		58.0%		23.9%	18.1%	
3N...Cl <sup>-</sup>	-36.36	50.67	-20.42	-20.46	-27.20	-47.28	45.44	-20.42	-12.72	-44.85
	47.1%		26.4%	26.5%		58.8%		25.4%	15.8%	
3N...Br <sup>-</sup>	-30.58	42.97	-15.73	-18.95	-23.05	-37.40	35.27	-15.61	-11.55	-36.94
	46.9%		24.1%	29.0%		57.9%		24.2%	17.9%	
3N...I <sup>-</sup>	-28.24	40.17	-11.84	-18.49	-18.49	-29.00	27.24	-11.76	-10.58	-29.04
	48.2%		20.2%	31.6%		56.5%		22.9%	20.6%	

### Energy decomposition analysis

Based on the above analysis, the experimental observations and the calculated interaction energies can provide the possible explanation for understanding the nature of intermolecular noncovalent interactions. In order to better unveiling the origin of the interactions, SAPT method was used to decompose the total interaction energy ( $E_{\text{SAPT}}$ ) into physically meaningful components for the complexes in gas phase, *i.e.*, electrostatic energy ( $E_{\text{elst}}$ ), exchange repulsion energy ( $E_{\text{exch}}$ ), induction energy ( $E_{\text{ind}}$ ) including the charge-transfer energy, as well as dispersion energy ( $E_{\text{disp}}$ ).<sup>23</sup> The energy decomposition results shows that the values of total interaction energy obtained by SAPT method are similar with that obtained by M06-2X/6-311++G(d,p)/LANL2DZdp ECP level, as listed in **Table 4**. Moreover, it can be noticed that the electrostatic energies are all greater than the corresponding induction and dispersion energies in the two bonding modes of 3CIN...X<sup>-</sup> and 3N...X<sup>-</sup> systems. The largest contributions to the total interaction energy are electrostatic term (the proportion of  $E_{\text{elst}}$  is 47% – 59%). In other words, the most important

contribution is electrostatic attraction. The other interaction energy terms contribute less to the total interaction energy (the proportion of  $E_{\text{ind}}$  and  $E_{\text{disp}}$  are 18% – 28% and 15% – 32%, respectively), but they cannot be ignored in the stabilization of the complexes.

### Natural Bond Orbital (NBO) analysis

Although the polarization/induction term contains the charge-transfer component in SAPT method, the specific contribution of charge-transfer cannot be obtained. In order to quantitatively evaluate the contribution of it involved in the formation of complexes, the NBO analysis was carried out for the two bonding models of complexes in the gas and solution phase. The NBO analysis stresses the role of intermolecular orbital interactions in the complexes, especially charge transfer.<sup>43,44</sup> The charge transfer occurs between the two molecules accompanied with the intermolecular orbital interactions.<sup>45</sup> The contribution of charge-transfer can be determined by the amount of charge transfer ( $\Delta q$ , *a.u.*) and the stabilization energy ( $E^2$ ). The stabilization energy refers to the delocalization degree of the electron density from the

**Table 5** The donor–acceptor interactions, second–order perturbation stabilization energies  $E^2$  (in  $\text{kJ}\cdot\text{mol}^{-1}$ ) and the amount of charge transfer  $\Delta q$  (in *a.u.*) of the  $\pi$ -hole and  $\sigma$ -hole bonding complexes in gas (G) and liquid (L) phase by NBO analysis.

		Donors	Acceptors	$E^2_{\text{total}}$	$\Delta q$
$\pi$ B complexes	3CIN...Cl <sup>-</sup>	LP(Cl <sup>-1</sup> )	BD*(C–N)	9.03(G)	0.0211(G)
				5.22(L)	0.0068(L)
	3CIN...Br <sup>-</sup>	LP(Br <sup>-1</sup> )	BD*(C–N)	8.28(G)	0.0192(G)
				4.48(L)	0.0063(L)
	3CIN...I <sup>-</sup>	LP(I <sup>-1</sup> )	BD*(C–N)	6.66(G)	0.0188(G)
				3.86(L)	0.0079(L)
	3N...Cl <sup>-</sup>	LP(Cl <sup>-1</sup> )	BD*(C–N)	3.69(G)	0.0111(G)
				1.30(L)	0.0020(L)
	3N...Br <sup>-</sup>	LP(Br <sup>-1</sup> )	BD*(C–N)	2.96(G)	0.0091(G)
				1.30(L)	0.0023(L)
	3N...I <sup>-</sup>	LP(I <sup>-1</sup> )	BD*(C–N)	2.47(G)	0.0101(G)
				1.26(L)	0.0042(L)
$\sigma$ B complexes	3CIN...Cl <sup>-</sup>	LP(Cl <sup>-1</sup> )	BD*(C–Cl)	25.19(G)	0.0463(G)
				8.00(L)	0.0100(L)
	3CIN...Br <sup>-</sup>	LP(Br <sup>-1</sup> )	BD*(C–Cl)	21.97(G)	0.0443(G)
				7.66(L)	0.0110(L)
	3CIN...I <sup>-</sup>	LP(I <sup>-1</sup> )	BD*(C–Cl)	17.82(G)	0.0436(G)
				7.66(L)	0.0138(L)
	3N...Cl <sup>-</sup>	LP(Cl <sup>-1</sup> )	BD*(C–H)	48.49(G)	0.0359(G)
				17.86(L)	0.0109(L)
	3N...Br <sup>-</sup>	LP(Br <sup>-1</sup> )	BD*(C–H)	35.60(G)	0.0284(G)
				16.32(L)	0.0104(L)
	3N...I <sup>-</sup>	LP(I <sup>-1</sup> )	BD*(C–H)	26.86(G)	0.0256(G)
				16.44(L)	0.0129(L)

"LP" for 1-center valence lone pair and "BD\*" for 2-center antibond.

bonding orbital to the antibonding (unoccupied) orbital. The calculated data are listed in **Table 5**. Taking the gas phase as example, the charge transfer of the  $\pi$ -hole...X<sup>-</sup> bond is observed from the lone pair electrons of X<sup>-</sup> to the antibonding orbital (BD\*C–N) of C–N bond. And the amounts of charge–transfer are 0.0188 – 0.0211 *a.u.* and 0.0091 – 0.0111 *a.u.* for the 3CIN...X<sup>-</sup> and 3N...X<sup>-</sup>  $\pi$ -hole bonding complexes, respectively. The charge transfer of the  $\sigma$ -hole...X<sup>-</sup> bond is observed from the lone pair electrons of X<sup>-</sup> to the antibonding orbital (BD\*C–Cl/H) of C–Cl or C–H bond. The corresponding amounts of charge–transfer are 0.0436 – 0.0463 *a.u.* and 0.0256 – 0.0359 *a.u.* for 3CIN...X<sup>-</sup> and 3N...X<sup>-</sup>  $\sigma$ -hole bonding complexes, respectively. In addition, the calculated  $E^2$  are 6.66 – 9.03  $\text{kJ}\cdot\text{mol}^{-1}$  and 2.47 – 3.69  $\text{kJ}\cdot\text{mol}^{-1}$  for 3CIN...X<sup>-</sup> and 3N...X<sup>-</sup>  $\pi$ -hole bonding complexes, and the values are 17.82 – 25.19  $\text{kJ}\cdot\text{mol}^{-1}$  and 26.86 – 48.49  $\text{kJ}\cdot\text{mol}^{-1}$  for the 3CIN...X<sup>-</sup> and 3N...X<sup>-</sup>  $\sigma$ -hole bonding complexes, respectively. Evidently, the values of  $\Delta q$  and  $E^2$  for the  $\pi$ -hole bonding complexes are all much smaller than the corresponding ones for the  $\sigma$ -hole bonding complexes both in gas phase and in liquid phase. Namely, the contribution of the charge–transfer term to the stabilization energy is larger in the  $\sigma$ -hole bonding complexes than in the  $\pi$ -hole bonding complexes.

#### Discussion

Based on the above experimental and calculation analysis, it can be shown that the bonding abilities of 3CIN and 3N to X<sup>-</sup>

follow the order of I<sup>-</sup> > Br<sup>-</sup> > Cl<sup>-</sup> in both titration experiments with high concentration of X<sup>-</sup> and solution–phase calculation, apparently the order of charge–transfer ability. While the bonding abilities present the reverse sequence in the gas–phase calculation, *i.e.*, an electrostatic ability sequence of halide anions.

The nature of the  $\pi$ -/ $\sigma$ -hole...X<sup>-</sup> bonds can be more accurately understood by calculation in gas phase because the interaction of donor with acceptor is unaffected by other external factors. While there is either weak or strong solvation in the spectroscopic titration experiments, and consideration of the solvation factor, PCM model, in the solution–phase calculation is more close to real experimental condition.

What reasons result in the different order in interaction strength? Is the nature of the  $\pi$ -/ $\sigma$ -hole...X<sup>-</sup> bond electrostatically dominative or charge–transfer dominative?

First of all, the recalled related literatures must be able to provide some useful information. In the aspect of the  $\pi$ -hole bond, Kochi *et al.*<sup>46</sup> explored the recognition abilities of several  $\pi$ -hole bonding donors to halide anions using UV spectral titration. Taking pyrazine–2,3,5,6–tetracarbonitrile (TCP) as an  $\pi$ -hole bonding donor, the association constants of TCP...Br<sup>-</sup>/I<sup>-</sup> complexes are 7 and 3 M<sup>-1</sup>, respectively, by setting the concentration of TCP at 5 mM with a variation of Br<sup>-</sup>/I<sup>-</sup> concentration from 0 to 208 mM in acetonitrile. That is, the bonding abilities of TCP to Br<sup>-</sup>/I<sup>-</sup> using the  $\pi$ -hole...X<sup>-</sup> bond obey the order of Br<sup>-</sup> > I<sup>-</sup>. Berryman and co-workers<sup>47</sup>

synthesized a di-donor host molecule with an amino-hydrogen and perfluorophenyl ring. The association constants obtained using  $^1\text{H}$  NMR spectroscopic titration experiments in  $\text{CDCl}_3$  are 30 ( $\text{Cl}^-$ ), 20 ( $\text{Br}^-$ ) and 34 ( $\text{I}^-$ )  $\text{M}^{-1}$ , which are monitored by adding the aliquots from stock solution of  $\text{Bu}_4\text{N}^+\text{X}^-$  (60 – 200 mM) to the solution of di-donor molecule (9 – 25 mM). The result indicates that the bonding ability follows the order  $\text{I}^- > \text{Cl}^- > \text{Br}^-$ . They used then a neutral  $\pi$ -hole bonding donor (1,3,5-tris(3,5-dinitrobenzoatomethyl)-2,4,6-triethylbenzene) with tripodal structure.<sup>48</sup>  $^1\text{H}$  NMR spectroscopic titrations confirmed that the donor exhibits the strongest interactions with  $\text{Cl}^-$  followed by  $\text{Br}^-$  and  $\text{I}^-$ , which was performed upon addition of  $\text{Bu}_4\text{N}^+\text{X}^-$  (from 0 – 120 mM) to 2 mM donor solution in  $\text{C}_6\text{D}_6$ . The measured association constants are 53 ( $\text{Cl}^-$ ), 35 ( $\text{Br}^-$ ) and 26 ( $\text{I}^-$ )  $\text{M}^{-1}$ , respectively. In addition, Wang *et al.*<sup>49</sup> developed a system of macrocyclic heteroatom-bridged heteroaromatic calixarenes, tetraoxacalix[2]arene[2]triazine (R = Cl), and studied its recognition abilities to halide anions using UV-Vis and fluorescence spectroscopic titration methods. The results from fluorescence titration show that the bonding abilities of macrocyclic donor molecule with  $\text{Bu}_4\text{N}^+$  salts decreased in the order  $\text{Cl}^- > \text{F}^- \gg \text{Br}^-$  (the corresponding association constants are 4246, 4036  $\text{M}^{-1}$  and none, respectively), which was performed upon addition of  $\text{Bu}_4\text{N}^+\text{X}^-$  (from 0 – 0.258 mM) to 1.74 mM donor solution in acetonitrile.

In the aspect of the  $\sigma$ -hole bond, Kochi *et al.*<sup>50</sup> studied the interactions between  $\text{CBr}_4/\text{CHBr}_3$  and halide anions using UV spectroscopy titration method which is carried out by an incremental addition of  $\text{Pr}_4\text{N}^+\text{X}^-$  (from 0 to 96 mM) to 7.5 mM  $\text{CBr}_4$  solution. The typical association constants of  $\text{CBr}_4$  and  $\text{X}^-$  (X = Cl, Br, I) in  $\text{CH}_2\text{Cl}_2$  solution were 3.0, 2.8 and 3.2  $\text{M}^{-1}$ , respectively, indicating the association ability obeys the order of  $\text{I}^- > \text{Cl}^- > \text{Br}^-$ , but actually similar. Shen *et al.*<sup>51</sup> studied the strong  $\text{C-I}\cdots\text{X}^-$   $\sigma$ -hole bond of diiodoperfluoroalkanes (DIPFA) with halide anions in acetonitrile using different spectroscopy method. UV-Vis titration experiment, which was monitored by setting the concentration of  $\text{X}^-$  at 0.5 mM with a variation of DIPFA (1.0 – 20 mM), indicated that the same  $\sigma$ -hole bonding donor has different bonding abilities for  $\text{X}^-$ , that is,  $\text{Cl}^- > \text{Br}^- > \text{I}^-$ . Taking 1,6-diiodoperfluorohexane as an example, the association constants are 251.7 ( $\text{Cl}^-$ ), 149.2 ( $\text{Br}^-$ ) and 81.3 ( $\text{I}^-$ )  $\text{M}^{-1}$ , respectively. However, the redshifts of the infrared vibrational frequencies and variations of chemical shift in the  $^{19}\text{F}$  NMR and  $^{13}\text{C}$  NMR (the concentration of DIPFA and  $\text{Bu}_4\text{N}^+\text{X}^-$  were all set at 0.1 M) followed the order  $\text{I}^- > \text{Br}^- > \text{Cl}^-$ , which is contrary with the result obtained from UV-Vis titration. Resnati *et al.*<sup>52</sup> confirmed that variations of chemical shift in the  $^{19}\text{F}$  NMR also followed the order  $\text{I}^- > \text{Br}^- > \text{Cl}^-$  after adding the  $\text{ICF}_2\text{CF}_2\text{I}$  (0.035 M) to the same concentration of  $\text{Bu}_4\text{N}^+\text{X}^-$  (0.098 M) in  $\text{CDCl}_3$  solution. The corresponding values of the  $^{19}\text{F}$  NMR shift variations ( $\Delta\delta$ ) were 2.17, 3.10 and 3.54 ppm, respectively. In addition, in crystals,  $d_{\text{Br-X}}$  ( $\text{\AA}$ ) in  $\text{C-Br}\cdots\text{Cl}^-$  3.190 (0.57), in  $\text{C-Br}\cdots\text{Br}^-$  3.207 (0.69), in  $\text{C-Br}\cdots\text{I}^-$  3.294 (0.82), force constants  $K$  ( $\text{mdyn \AA}^{-1}$ ), 0.10 – 0.14 in  $\text{C-Br}\cdots\text{Cl}^-$ , 0.13 –

0.15 in  $\text{C-Br}\cdots\text{Br}^-$ , 0.17 – 0.19 in  $\text{C-Br}\cdots\text{I}^-$ , this is the order for real charge-transfer interaction.<sup>53</sup>

It can be noticed from above reports in literatures and results obtained herein by experiments and calculation that the strength order of the  $\pi$ - $\sigma$ -hole...halide bond actually depends on two factors except geometric matching between host and halide, one is the ability of the  $\pi$ - $\sigma$ -hole...halide bond *per se*, another is solvent effect. For the strong  $\pi$ - $\sigma$ -hole...halide bond in the solvents with weak or middle polarity, the order should be electrostatically dominant, *i.e.*,  $\pi$ - $\sigma$ -hole... $\text{Cl}^- > \pi$ - $\sigma$ -hole... $\text{Br}^- > \pi$ - $\sigma$ -hole... $\text{I}^-$  in bonding ability. For the weak  $\pi$ - $\sigma$ -hole...halide bond in the solvents with middle or strong polarity or strong  $\pi$ - $\sigma$ -hole...halide bond in strong polar solvent, the order should be  $\pi$ - $\sigma$ -hole... $\text{I}^- > \pi$ - $\sigma$ -hole... $\text{Br}^- > \pi$ - $\sigma$ -hole... $\text{Cl}^-$ . Apparently it is a sequence of charge transfer ability, but actually the reason is the competition between the  $\pi$ - $\sigma$ -hole... $\text{X}^-$  bond and solvation of anion or anionic hydrogen bond between solvent molecule and halide.

$\text{Cl}^-$  has higher solvation free energy than  $\text{Br}^-$  and  $\text{I}^-$ , for example, they are 253.6, 236.8 and 213.0  $\text{kJ}\cdot\text{mol}^{-1}$ , respectively, in acetonitrile.<sup>54</sup> Also the hydration free energy trends of three ions is  $\text{Cl}^-$  (419.7  $\text{kJ}\cdot\text{mol}^{-1}$ )  $>$   $\text{Br}^-$  (394.1  $\text{kJ}\cdot\text{mol}^{-1}$ )  $>$   $\text{I}^-$  (358.6  $\text{kJ}\cdot\text{mol}^{-1}$ ), respectively.<sup>55</sup> Moreover, the experiment and calculation showed that the ionic hydrogen-bond of iodide is weakest for this largest halide of the series.<sup>56</sup> Therefore, the  $\sigma$ -hole bond and  $\pi$ -hole bond compete with solvation and possible anion-hydrogen bond between solvent molecule and halide in solution. A tradeoff is that the apparent charge transfer order of  $\pi$ - $\sigma$ -hole... $\text{I}^- > \pi$ - $\sigma$ -hole... $\text{Br}^- > \pi$ - $\sigma$ -hole... $\text{Cl}^-$  occurs for the weak  $\pi$ -hole bond and  $\sigma$ -hole bond, while really electrostatic attractive order of  $\pi$ - $\sigma$ -hole... $\text{Cl}^- > \pi$ - $\sigma$ -hole... $\text{Br}^- > \pi$ - $\sigma$ -hole... $\text{I}^-$  works for the strong ones. The order  $\pi$ - $\sigma$ -hole... $\text{I}^- > \pi$ - $\sigma$ -hole... $\text{Br}^- > \pi$ - $\sigma$ -hole... $\text{Cl}^-$  obtained by experiments does not affect the conclusion that the nature of the interaction is electrostatically attractive.

## Conclusions

The  $^{13}\text{C}$  NMR chemical shift moving to higher field indicated that the main bonding model was the  $\pi$ -hole... $\text{X}^-$  bond between 3CIN/3N processing both the  $\sigma$ -hole and  $\pi$ -hole and  $\text{X}^-$ . That is, there is competitive effect between the  $\sigma$ -hole bond and  $\pi$ -hole bond. Furthermore, the optimized geometric structures and interaction energies of the 3CIN/3N... $\text{X}^-$  complexes in both the  $\sigma$ -hole and  $\pi$ -hole bonding models were obtained using computational chemistry. The calculation results show that the bonding abilities in solution phase were essentially consistent with that obtained by titration experiments, *i.e.*,  $\text{I}^- > \text{Br}^- > \text{Cl}^-$ , apparently, it obeys a charge transfer sequence. However, the bonding abilities present the reverse sequence in the gas phase, *i.e.*,  $\text{Cl}^- > \text{Br}^- > \text{I}^-$ . Actually, it is a tradeoff between the  $\pi$ - $\sigma$ -hole... $\text{X}^-$  and solvation of anions and possible anionic hydrogen bond between solvent molecule and halide. However, in nature, the  $\pi$ - $\sigma$ -hole... $\text{X}^-$  still is electrostatically attractive, which is supported by SAPT

energy decomposition analysis, and the induction and dispersion interactions play a minor role in the stabilization of the complexes. NBO analysis further confirms that there is minimal contribution of the charge-transfer term to the formation of complexes. All these results provide significant references for designing and synthesizing the novel supramolecular host molecules or sensors to selectively recognize anions based on the competition of the  $\pi$ -hole bond and  $\sigma$ -hole bond or  $\pi$ -/ $\sigma$ -hole bond with solvation.

### Acknowledges

The authors thank the Natural Science Foundation of China (No.90922023 and No.21173113) and the State Key Laboratory of Environmental Chemistry and Ecotoxicology, Research Center for Eco-Environmental Sciences, Chinese Academy of Sciences (KF2013-21) for the supports.

### References

- 1 C. Suksai and T. Tuntulani, *Chem. Soc. Rev.*, 2003, **32**, 192.
- 2 F. P. Schmidtchen, *Top. Curr. Chem.*, 2005, **255**, 1.
- 3 P. Politzer, J. S. Murray and T. Clark, *Phys. Chem. Chem. Phys.*, 2013, **15**, 11178.
- 4 A. Priimagi, G. Cavallo, P. Metrangolo and G. Resnati, *Acc. Chem. Res.*, 2013, **46**, 2686.
- 5 H. T. Chifotides and K. R. Dunbar, *Acc. Chem. Res.*, 2013, **46**, 894.
- 6 A. Bauz, T. J. Mooibroek and A. Frontera, *ChemPhysChem*, 2015, DOI: 10.1002/cphc.201500314
- 7 Z. P. Shields, J. S. Murray and P. Politzer, *Int. J. Quantum Chem.*, 2010, **110**, 2823.
- 8 M. S. Taylor, *Nat. Chem.*, 2014, **6**, 1029.
- 9 S. W. Robinson, C. L. Mustoe, N. G. White, A. Brown, A. L. Thompson, P. Kennepohl and P. D. Beer, *J. Am. Chem. Soc.*, 2015, **137**, 499.
- 10 S. T. Schneebeli, M. Frasconi, Z. C. Liu, Y. L. Wu, D. M. Gardner, N. L. Strutt, C. Y. Cheng, R. Carmieli, M. R. Wasielewski and J. F. Stoddart, *Angew. Chem. Int. Ed.*, 2013, **52**, 13100.
- 11 Q. He, Z. T. Huang and D. X. Wang, *Chem Commun.*, 2014, **50**, 12985.
- 12 D. Y. Kim, N. J. Singh and K. S. Kim, *J. Chem. Theory Comput.*, 2008, **4**, 1401.
- 13 Q. Z. Li, R. Li, X. F. Liu, W. Z. Li and J. B. Cheng, *ChemPhysChem*, 2012, **13**, 1205.
- 14 K. E. Riley, J. S. Murray, J. Fanfrlík, J. Řezáč, R. J. Solá, M. C. Concha, F. M. Ramos and P. Politzer, *J. Mol. Model.*, 2013, **19**, 4651.
- 15 Z. A. Tehrani, Z. Jamshidi and H. Farhangian, *J. Mol. Model.*, 2013, **19**, 4763.
- 16 P. Deepa, R. Sedlak and P. Hobza, *Phys. Chem. Chem. Phys.*, 2014, **16**, 6679.
- 17 I. Alkorta, I. Rozas and J. Elguero, *J. Am. Chem. Soc.*, 2002, **124**, 8593.
- 18 D. Quiñonero, C. Garau, C. Rotger, A. Frontera, P. Ballester, A. Costa and P. M. Deyà, *Angew. Chem. Int. Ed.*, 2002, **41**, 3389.
- 19 C. Garau, A. Frontera, D. Quiñonero, P. Ballester, A. Costa and P. M. Deyà, *ChemPhysChem*, 2003, **4**, 1344.
- 20 D. Kim, P. Tarakeshwar and K. S. Kim, *J. Phys. Chem. A*, 2004, **108**, 1250.
- 21 Q. Z. Li, R. Li, X. F. Liu, W. Z. Li and J. B. Cheng, *J. Phys. Chem. A*, 2012, **116**, 2547.
- 22 L. P. Wolters and F. M. Bickelhaupt, *ChemistryOpen*, 2012, **1**, 96.
- 23 K. E. Riley and P. Hobza, *J. Chem. Theory Comput.*, 2008, **4**, 232.
- 24 K. E. Riley and P. Hobza, *Phys. Chem. Chem. Phys.*, 2013, **15**, 17742.
- 25 P. Deepa, B. V. Pandiyan, P. Kollandaivel and P. Hobza, *Phys. Chem. Chem. Phys.*, 2014, **16**, 2038.
- 26 Y. Zhao and D. G. Truhlar, *Theor. Chem. Acc.*, 2008, **120**, 215.
- 27 A. Bauzá, I. Alkorta, A. Frontera and J. Elguero, *J. Chem. Theory Comput.*, 2013, **9**, 5201.
- 28 V. Barone and M. Cossi, *J. Phys. Chem. A*, 1998, **102**, 1995.
- 29 A. J. Misquitta, R. Podeszwa, B. Jeziorski and K. Szalewicz, *J. Chem. Phys.*, 2005, **123**, 214103.
- 30 A. J. Misquitta and K. Szalewicz, *J. Chem. Phys.*, 2005, **122**, 214109.
- 31 A. E. Reed, L. A. Curtiss and F. Weinhold, *Chem. Rev.*, 1988, **88**, 899.
- 32 M. J. Frisch, G. W. Trucks, H. B. Schlegel, G. E. Scuseria, M. A. Robb, J. R. Cheeseman, G. Scalmani, V. Barone, B. Mennucci, G. A. Petersson, H. Nakatsuji, M. Caricato, X. Li, H. P. Hratchian, A. F. Izmaylov, J. Bloino, G. Zheng, J. L. Sonnenberg, M. Hada, M. Ehara, K. Toyota, R. Fukuda, J. Hasegawa, M. Ishida, T. Nakajima, Y. Honda, O. Kitao, H. Nakai, T. Vreven, J. A. Montgomery, Jr., J. E. Peralta, F. Ogliaro, M. Bearpark, J. J. Heyd, E. Brothers, K. N. Kudin, V. N. Staroverov, R. Kobayashi, J. Normand, K. Raghavachari, A. Rendell, J. C. Burant, S. S. Iyengar, J. Tomasi, M. Cossi, N. Rega, J. M. Millam, M. Klene, J. E. Knox, J. B. Cross, V. Bakken, C. Adamo, J. Jaramillo, R. Gomperts, R. E. Stratmann, O. Yazyev, A. J. Austin, R. Cammi, C. Pomelli, J. W. Ochterski, R. L. Martin, K. Morokuma, V. G. Zakrzewski, G. A. Voth, P. Salvador, J. J. Dannenberg, S. Dapprich, A. D. Daniels, Ö. Farkas, J. B. Foresman, J. V. Ortiz, J. Cioslowski and D. J. Fox, *GAUSSIAN 09*, Gaussian, Inc., Wallingford, CT, 2009.
- 33 H. J. Werner, P. J. Knowles, G. Knizia, F. R. Manby, M. Schütz, P. Celani, T. Korona, R. Lindh, A. Mitrushenkov, G. Rauhut, K. R. Shamasundar, T. B. Adler, R. D. Amos, A. Bernhardsson, A. Berning, D. L. Cooper, M. J. O. Deegan, A. J. Dobbyn, F. Eckert, E. Goll, C. Hampel, A. Hesselmann, G. Hetzer, T. Hrenar, G. Jansen, C. Köppl, Y. Liu, A. W. Lloyd, R. A. Mata, A. J. May, S. J. McNicholas, W. Meyer, M. E. Mura, A. Nicklaß, D. P. O'Neill, P. Palmieri, D. Peng, K. Pflüger, R. Pitzer, M. Reiher, T. Shiozaki, H. Stoll, A. J. Stone, R. Tarroni, T. Thorsteinsson and M. Wang, *MOLPRO, version 2010.1*, Cardiff, UK, 2010.
- 34 R. S. Mulliken, *J. Am. Chem. Soc.*, 1952, **74**, 811.
- 35 R. S. Mulliken and W. B. Person, *Molecular complexes*, Wiley, New York, USA, 1969.
- 36 Y. J. Wu, X. R. Zhao, H. Y. Gao and W. J. Jin, *Chin. J. Chem. Phys.*, 2014, **27**, 265.
- 37 H. A. Benesi and J. H. Hildebrand, *J. Am. Chem. Soc.*, 1949, **71**, 2703.
- 38 N. Ma, Y. Zhang, B. M. Ji, A. M. Tian and W. Z. Wang, *ChemPhysChem*, 2012, **13**, 1411.
- 39 P. D. Rege, O. L. Malkina and N. S. Goroff, *J. Am. Chem. Soc.*, 2002, **124**, 370.
- 40 W. N. Moss and N. S. Goroff, *J. Org. Chem.*, 2005, **70**, 802.
- 41 Y. Zhang, B. M. Ji, A. M. Tian and W. Z. Wang, *J. Chem. Phys.*, 2012, **136**, 141101.
- 42 Q. M. Mou, Y. Peng, Z. G. Zhao and S. H. Chen, *Chin. J. Org. Chem.*, 2004, **24**, 1018.
- 43 X. Y. Zhang, Y. L. Zeng, X. Y. Li, L. P. Meng and S. J. Zheng, *Struct. Chem.*, 2011, **22**, 567.
- 44 Z. X. Wang, B. S. Zheng, X. Y. Yu, X. F. Li and P. G. Yi, *J. Chem. Phys.*, 2010, **132**, 164104.

## Journal Name

## ARTICLE

- 45 Q. Z. Li, B. Jing, Z. B. Liu, W. Z. Li, J. B. Cheng, B. A. Gong and J. Z. Sun, *J. Chem. Phys.*, 2010, **133**, 114303.
- 46 Y. S. Rosokha, S. V. Lindeman, S. V. Rosokha and J. K. Kochi, *Angew. Chem. Int. Ed.*, 2004, **43**, 4650.
- 47 O. B. Berryman, F. Hof, M. J. Hynes and D. W. Johnson, *Chem. Commun.*, 2006, 506.
- 48 O. B. Berryman, A. C. Sather, B. P. Hay, J. S. Meisner and D. W. Johnson, *J. Am. Chem. Soc.*, 2008, **130**, 10895.
- 49 D. X. Wang, Q. Y. Zheng, Q. Q. Wang, and M. X. Wang, *Angew. Chem. Int. Ed.*, 2008, **47**, 7485.
- 50 S. V. Lindeman, J. Hecht and J. K. Kochi, *J. Am. Chem. Soc.*, 2003, **125**, 11597.
- 51 Q. J. Shen and W. J. Jin, *Phys. Chem. Chem. Phys.*, 2011, **13**, 13721.
- 52 R. Liantonio, P. Metrangolo, T. Pilati and G. Resnati, *Cryst. Growth Des.*, 2003, **3**, 355.
- 53 J. A. Creighton and K. M. Thomas, *J. Chem. Soc. Dalton Trans.*, 1972, 403.
- 54 M. H. Abraham and J. Liszi, *J. Chem. Soc., Faraday Trans. 1*, 1978, **74**, 1604.
- 55 M. Salomen, *J. Phys. Chem.*, 1970, **74**, 2519.
- 56 P. Ayotte, C. G. Bailey, G. H. Weddle, M. A. Johnson, *J. Phys. Chem. A*, 1998, **102**, 3067.